SCIENTIFIC REP⚙RTS

OPEN

Visible-light-accelerated oxygen vacancy migration in strontium titanate

Y. Li, Y. Lei, B. G. Shen & J. R. Sun

Strontium titanate is a model transition metal oxide that exhibits versatile properties of special interest for both fundamental and applied researches. There is evidence that most of the attractive properties of $SrTiO_3$ are closely associated with oxygen vacancies. Tuning the kinetics of oxygen vacancies is then highly desired. Here we reported on a dramatic tuning of the electro-migration of oxygen vacancies by visible light illumination. It is found that, through depressing activation energy for vacancy diffusion, light illumination remarkably accelerates oxygen vacancies even at room temperature. This effect provides a feasible approach towards the modulation of the anionic processes. The principle proved here can be extended to other perovskite oxides, finding a wide application in oxide electronics.

Strontium titanate ($SrTiO_3$, STO) is a model transition metal oxide, receiving intensive attentions due to its abundant physical properties. It is ordinarily paraelectric due to quantum fluctuation but undergoes a ferroelectric transition when stressed by lattice strains[1–3] or electrical field[4–6]; it is typically insulating but exhibits a resistive transition to electronically conducting[7], even to superconducting[8] when it is oxygen-deficient. Due to its versatile properties, it serves as battery[9], chemical sensors[10], photo-catalysts[11], and resistance-random-access-memory (RRAM) cell for non-volatile data storage[12]. Since most of these properties are closely related to the in- and ex-corporation reactions of oxygen, particularly the diffusion of oxygen vacancies (V_Os), tuning the ionic processes is then highly desired. We noted that most of the previous work focused more on understanding than on tuning of the kinetic behaviors of V_Os, and the interested issues include the forms of oxygen vacancies in STO (isolated V_O, V_O-pairs, or the V_O trapped by defect)[13–18], their influence on anionic diffusion[19,20], and spatial distribution of oxygen vacancies in STO[21,22]. Although there are attempts to modify the incorporation of oxygen[23] or to generate oxygen defects on STO surface through ultraviolet light irridiation[24], data in this regard are still very limited. The tuning of the kinetic behavior of V_Os remains challenging, required further exploration. Here we reported on a dramatic tuning of the mobility of oxygen vacancies in STO by visible light illumination. It was found that, through exciting in-gap states of STO, light illumination depresses the activation energy for vacancy diffusion, remarkably accelerating the diffusion of V_Os. Through speeding up ionic transport, this effect will find its applications in oxide electronics.

Results

Electrical field-induced and light illumination-accelerated structural deformation. As schemed in Fig. 1a, samples are (001)-orientated STO substrates of the dimension of $5 \times 5 \times 0.5\,mm^3$. As electrodes, two Ti layers were deposited respectively on the top and bottom surfaces through magnetron sputtering in an Ar atmosphere of 0.5 Pa. A gate voltage, V_G, between $-200\,V$ and $200\,V$ was applied to the back gate of STO while the top surface was grounded. In all cases, the leakage current is lower than 10 nA at the ambient temperature, which rules out the effect of Joule heating. Fig. 1b presents the x-ray diffraction (XRD) spectra of the 002 Bragg reflection of STO, recorded in the presence or absence of

Beijing National Laboratory for Condensed Matter & Institute of Physics, Chinese Academy of Sciences, Beijing 100190, Peoples' Republic of China. Correspondence and requests for materials should be addressed to J.R.S. (email: jrsun@iphy.ac.cn)
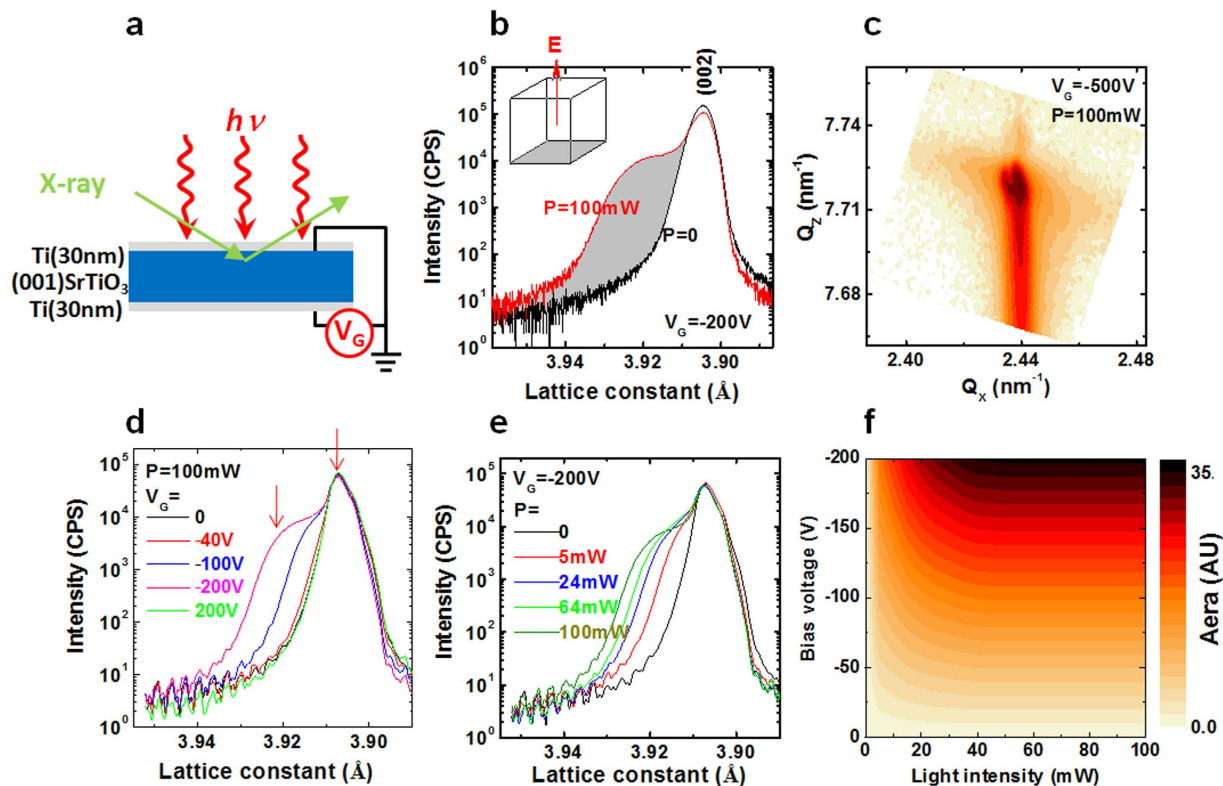
Figure 1. Effect of combined electrical and optical stimuli on the structure of STO. (a) A sketch of the experimental setup for x-ray diffraction. **(b)** XRD spectra of the 002 reflection of (001)-STO, recorded right upon the application of an electrical field along the [001]-axis. The duration of each $\vartheta-2\vartheta$ scanning is 180 s. Shaded area marks the difference of the two XRD spectra with and without light illumination. The inset sketch shows the field direction with respect to the axes of the unit cell. **(c)** A reciprocal mapping of the 103 reflection of STO, measured under the conditions of $V_G = -500$ V and $P = 100$ mW. The downward tail of the main reflection marks the c-axis lattice expansion. **(d)** Structural changes for a constant light illumination but different gate fields. Positive gate bias produces no effect on structure even aided by illumination. Arrows mark the positions of the Bragg reflections. **(e)** Structural changes with light power while gate voltage is kept constant. **(f)** Distribution of structural deformation on V_G-P plane, showing the combined effect of the electrical stressing and light illuminating. Light wavelength adopted here is $\lambda = 532$ nm. In all cases the leakage current is lower than 10 nA. All measurements were conducted at room temperature.

light. Without illumination, a bias voltage up to ± 200 V produces negligible effects on the structure of STO. This can be ascribed to the low mobility of oxygen vacancies ($\sim 8 \times 10^{-12}$ cm^2/Vs at room temperature[20]).As recently reported, the structural deformation only occurs for STO accompanying the electro-migration of V$_O$s[6]. It is easy to calculate the time required for the V$_O$s to drift out of the interfacial layer, and it is ~ 6200 s under the gate bias of -200 V if layer thickness is $\sim 2\mu$m, well beyond the time window of the $\vartheta-2\vartheta$ scanning (~ 180 s). Aided by light, however, a gate bias of -200 V is high enough to cause sizable structural deformation. As shown in Fig. 1b, an obvious shoulder appears beside the main reflection when illuminated by a light of $P = 100$ mW ($\lambda = 532$ nm), indicating a lattice expansion along [001] axis. Since the unchanged phase can be clearly seen, the deformed phase could be much thinner than the penetration depth of x-ray in STO ($\sim 6\mu$m), appearing in an interfacial layer. According to reciprocal space mapping of the 103 reflection, fascinatingly, this new phase has an elongated c-axis lattice constant but a unchanged a-axis one (Fig. 1c). In contrast, positive biases produce no effect on lattice even aided by illumination, which means that the field-induced lattice expansion only appears underneath anode (Fig. 1d).

For a thorough exploration of this new gating effect, we measured the XRD spectra for various combinations of V_G and P. Fixing P to 100 mW while varying V_G, according to Fig. 1d, lattice expansion emerges when V_G exceeds -40 V. From $V_G = -40$ V to -200 V, the lattice constant changes from 3.905 Å to 3.922 Å (marked by red arrows), increasing by $\sim 0.4\%$. While fixing V_G to -200 V but tuning P, sizable gating effect appears when $P = 5$ mW (Fig. 1e), i.e., the structural distortion caused by the gating effects can be accelerated remarkably even in low light power. Quantifying the lattice expansion in Fig. 1b by a shaded area, we obtain a quantitative description of the gating effects in the V_G-P plane (Fig. 1f),
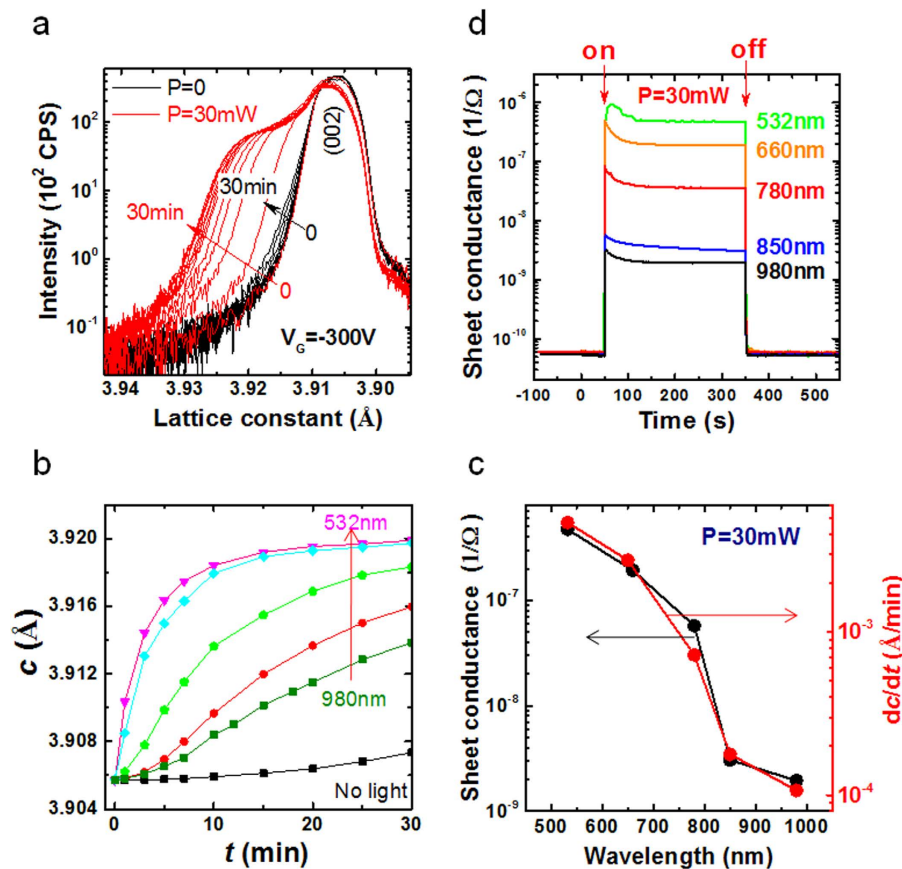
Figure 2. Concomitant variation in sheet conductance and structural deformation. (**a**) Evolution of the 002 reflection of STO with gating time, where $V_G = -300$ V, $P = 0$ or 30 mW, and $\lambda = 532$ nm. (**b**) Lattice constant as a function of time, where $V_G = -300$ V, $P = 0$ or 30 mW, and λ varies between 532 nm and 980 nm. (**c**) Sheet conductance of the LAO(3uc)/STO interface corresponding to the light ON/OFF operation, where $P = 30$ mW and λ varies between 532 nm and 980 nm. The applied current for resistive measurement is $1\,\mu$A. (**d**) A comparison of sheet conductance and structural change. Solid lines are guides for the eye. All measurements were performed at room temperature.

clearly showing the combined effects of gate field and light illumination. As suggested in ref. 6, structural deformation occurs accompanying the electro-migration of V_Os, these results suggest a mobilization of oxygen vacancies by light illuminating.

Photo-excitation-modulated lattice expansion.   To reveal the effect of light illumination, the evolution of the 002 reflection with time is recorded when STO is exposed to different lights in the presence of electrical bias. Figure 2a shows the XRD spectra for two typical cases of $P = 0$ and 30 mW ($\lambda = 532$ nm, $V_G = -300$ V). Figure 2b is a summary of the data for different wavelengths ($P = 30$ mW). As shown in Fig. 2b, the acceleration of short wavelength light to gating effect is prompt: Lattice expansion occurs right upon the application of V_G and completes within about 10 minutes. Increasing λ leads to an inclining of the $c(t)$ curve, indicating a slowdown of the gating effect. To get a quantitative description of the wavelength effect, in Fig. 2c we present, in semi-logarithmic scale, the dependence of dc/dt on λ, derived from the $c(t)$ curve in the initial stage of structural deformation. A simple calculation shows that dc/dt is ~0.0047 Å/min for $\lambda = 532$ nm and ~0.0001 Å/min for $\lambda = 980$ nm, depressing nearly 50-fold.

The distinctive $dc/dt - \lambda$ relation implies that the acceleration of the gating effect may be ascribed to photo-excitation rather than thermal activation. This is understandable since the photon energy used in the present experiments is well beyond the range of phonon energy. In fact, a direct effect of photo-excitation could be observed on photoconductivity. Since STO is insulating, its photoconductivity cannot be directly measured with visible light. We choose a LaAlO$_3$/SrTiO$_3$ interface with a 3-unit-cell-thick LaAlO$_3$ top layer as a sample. As well established[25], the interface will be insulating when the LaAlO$_3$ layer is thinner than 4 unit cells for lack of mobile sheet charge carriers. However, we found that this insulating interface can be driven into conductive state by illuminating. As exemplified by Fig. 2d, from $\lambda = 532$ nm to 980 nm ($P = 30$ mw), the sheet conductance changes from $G \approx 2 \times 10^{-5}\Omega^{-1}$ to ~$6 \times 10^{-8}\Omega^{-1}$. It is obvious that light illumination generates extra charge carriers by exciting the
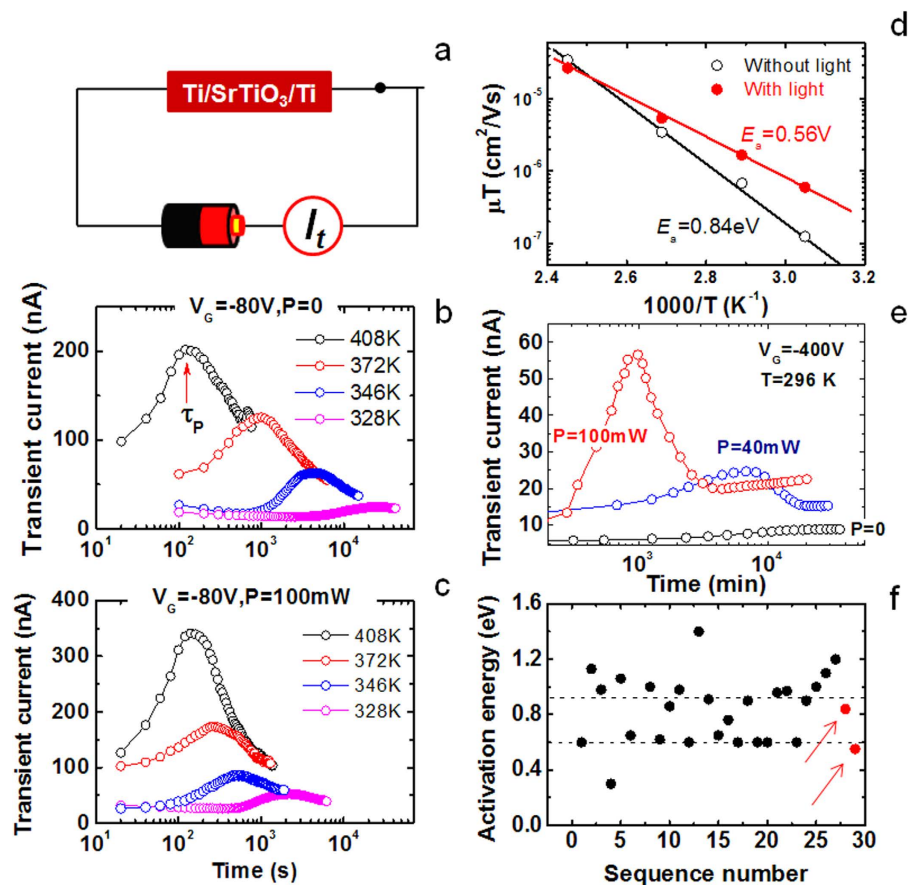
Figure 3. Transient current through biased STO. (**a**) A sketch of the experimental setup for transient current measurements. (**b**) Transient current for $V_G = -80$ V and $P = 0$, measured under different temperatures. Arrow marks the position of current peak. (**c**) Transient current for $V_G = -80$ V and $P = 100$ W ($\lambda = 532$ nm). (**d**) Semi-logarithmic plot of the vacancy mobility against reciprocal temperature. Solid lines are guides for the eye. (**e**) Transient current measured under different light powers ($V_G = -400$ V, $\lambda = 532$ nm). (**f**) Activation energies of oxygen vacancies obtained by different groups (refs 18–20). Our results are represented by two red symbols (marked by two arrows). Dashed lines are guides for the eye.

in-gap states of STO (photon energy is lower than the band gap of STO), leading to the growth of sheet conductance. When the quantum efficiency for photo-excitation decreases with the increase of λ, G accordingly decreases. Surprisingly, the G-λ relation mimics the dc/dt-λ dependence very well, even in detailed features (Fig. 2c). This result strongly suggests that it is the photo-excitation of the in-gap states of STO that accelerates the gating effect. We noted that the light illumination induced conductance enhancement has been observed previously[26,27]. These works revealed the photo-excitation-generated effect. According to our data, we believed that photo-excitation of the in-gap state of STO, which gives rise to photoconductivity as shown in Fig. 2d, causes a transition of $V_O^{\bullet}$ to $V_O^{\bullet\bullet} + e$, accelerating vacancy diffusion, as will be discussed later.

Illumination-accelerated oxygen vacancies. A further question is how photo-excitation accelerates the gating effect. As suggested by Hanzig *et al.*[6], the structural deformed phase forms while oxygen vacancies drift along electric field. In this scenario, photo-excitation may affect the gating effect through accelerating vacancy diffusion. To reveal the effect of light illumination on oxygen vacancies, transient current, $i(t)$, through an electrically biased STO is studied in the presence (absence) of light illumination. Figure 3a is a schematic experimental setup. Figure 3b,c display the transient current as a function of time, recorded by fixing V_G to -80 V at a temperature between 328 K and 408 K. With the increase of t, the transient current undergoes first a low to high and then a high to low transition, leaving a current peak at τ_P. This feature is observed in all $i(t)$ curves acquired at different temperatures. Comparing with the data without light, we found that light illumination causes an obvious left shift of current peak. This phenomenon is particularly evident when temperature is not very high. For example, at a temperature of 328 K, τ_P is ~2100 s in light but ~24970 s without light, i.e., the time required to reach the current peak has been reduced by more than one order of magnitude by light illumination. This result implies

an acceleration of vacancy diffusion. As well established, the transient current is carried by V_Os, and the transient current gets a maximum when the oxygen vacancies underneath anode arrive at cathode[6,28].

As predicted by space-charge-limited (SCL) theory, the peak position of $i(t)$ has a close relation to the mobility, μ, of oxygen vacancies following the equation[28,29].

$$\tau_p = 0.78d^2/\mu V_G, \tag{1}$$

where d is the thickness of the sample. If the transient current is exclusively due to ionic charges, we will have the following equation

$$\mu = (\gamma q/k_B T)\exp(-E_A/k_B T), \tag{2}$$

where E_A is the activation energy for oxygen vacancy diffusion, k_B is the Boltzmann's constant, T is the temperature, q is the charge of oxygen vacancy, and γ is a pre-exponential factor. Here the Einstein relation between mobility and diffusivity, $\mu = qD/k_B T$, has been adopted for the derivation of Eq. (2). Based on Eq. (1), μ as a function of temperature can be deduced from the data in Fig. 3b,c. A direct calculation shows that the mobility is, for example, for $T = 328\,K$, $\sim 3.8 \times 10^{-10}\,cm^2/Vs$ without light and $\sim 1.8 \times 10^{-9}\,cm^2/Vs$ with light. Extrapolating the data in Fig. 3b,c to room temperature (296 K), we obtain the vacancy mobility of $\sim 1.8 \times 10^{-11}\,cm^2/Vs$ without light, which is comparable to the value deduced from ref. 20 ($\sim 8 \times 10^{-12}\,cm^2/Vs$).

Remarkably, the μ-T relation is well described by Eq. (2). This, in addition to confirming the ionic origin of the transient current, reveals the activation nature of the charge transport process. From the slope of the semi-logarithmic μT-T plot in Fig. 3d, the activation energy can be deduced. It is $\sim 0.84\,eV$ without light and $\sim 0.56\,eV$ in a light of, for example, 100 mW and 532 nm. Light illumination reduces E_A by $\sim 34\%$. These results indicate that, indeed, light illuminating mobilizes oxygen vacancies. Here we emphasize that the activation energy may be continuously depressed by illumination, as suggested by the progressive left shift of the current peak as P grows (Fig. 3e).

In fact, the diffusion of oxygen vacancies in STO has been intensively studied, and the activation energy obtained by different groups concentrated on two distinct categories around 0.6 eV and 1 eV (Fig. 3f)[19,20]. It is instructive to note that the activation energies deduced here (0.56 eV and 0.84 eV) also fall into these two groups (Fig. 3f). As will be discussed later, this may be an indication for illumination-induced changes in the V_O-complexes that are believed to widely exist in STO, and this could be the underlying reason for the mobilization of V_Os.

Discussions

The above experiments suggest that light illumination accelerates field-induced lattice expansion via accelerating oxygen vacancy diffusion (Figs 1 and 3), and this acceleration process occurs accompanying the photo-excitation of in-gap states of STO (Fig. 2). A further question is how oxygen vacancy diffusion related to photo-excitation.

In general, it is believed that oxygen vacancies are doubly ionized at high temperatures, existing in the form of isolated $V_O^{\bullet\bullet}$s[30]. According to Cordero[19], the binding energy of a V_O-complex is $\sim 0.2\,eV$. A direct calculation shows that the probability for a V_O-complex to be disassembled at 1000 °C is about 400-fold larger than that at 25 °C. At low temperatures, however, a singly ionized state could be favorable. By analyzing the relation between carrier concentration (n) and δ for $SrTiO_{3-\delta}$, Moos et al.[31] declared that oxygen vacancies were singly ionized near room temperature, i.e., each V_O donates one charge carrier in the meantime trapping an electron. In their experiments, a well linear $n-\delta$ relation was observed from $\delta = 0.03$ down to 0.01, without any signatures of inflection.

All of our experiments were conducted near room temperature. In this case, the content of singly ionized vacancies could be considerable. As well documented[15,16,19,30], singly ionized vacancies prefer to form V_O-complexes by sharing their electrons with the two closest titanium atoms, yielding in-gap states (Fig. 4a). In fact, V_O-complexes in the form of Ti^{3+}-V_O or V_O-Ti-V_O pairs have been proposed[13,15,16,19]. Presumably, the E_A of these V_O-complexes could be significantly larger than that of $V_O^{\bullet\bullet}$s (ref. 9). Various experiments have shown that E_A is $\sim 0.6\,eV$ for $V_O^{\bullet\bullet}$ and $\sim 1\,eV$ for V_O-complexes[15,19,20]. Since the photon energy used here is much lower than the band gap of STO, photo-illumination will only affect the V_O-complexes, exciting the shared electrons to the conduction band of STO. Without the shared electrons, however, the V_O-complexes become unstable, disassembling into isolated $V_O^{\bullet\bullet}$s (Fig. 4b). In this manner, photo-excitation accelerates the V_O diffusion thus the gating effect. This inference is in consistent with the observed illumination-induced reduction of E_A shown in Fig. 3d,f. To summarize, the present work reveals the close relation between photo-excitation and oxygen vacancy diffusion, paving the way towards the tuning of the anionic processes which could be important for oxide electronics.

Methods

Sample fabrication. Samples are (001)-oriented STO substrates ($5 \times 5 \times 0.5\,mm^3$) with an atomic level flat top surface. As electrodes, two 30-nm-thick Ti layers were deposited respectively on two surfaces through magnetron sputtering in an Ar atmosphere of 0.5 Pa. For comparison study, a $LaAlO_3$/$SrTiO_3$ sample with a $LaAlO_3$ overlayer (3 unit cells in thickness) was prepared using the pulsed laser
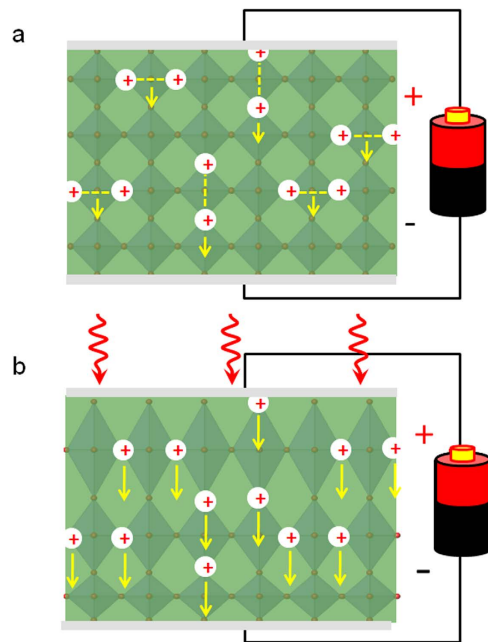
Figure 4. Schematic diagram for the migration of oxygen vacancies under electrical field and Light illumination. (a) Lattice deformation occurs accompanying the electro-migration of oxygen vacancies without light illumination. Oxygen vacancies near the STO surface may group into V_O-complexes (for example, V_O-Ti-V_O chains), and have a high activation energy for diffusion. As a consequence, the field-induced lattice change cannot be detected in the time window of the XRD experiments. **(b)** Photo-excitation of bounded electrons in the V_O-complex leads to the disassembly of the V_O-complexes, making oxygen vacancies much more mobile. Arrows mark the velocity of V_Os in electrical field.

(248 nm) ablation technique. In the deposition process, the temperature was kept at 800 °C and the oxygen pressure at 10^{-5} mbar. The fluence of the laser pulses was 0.7 Jcm^{-2}, and the repetition rate was 1 Hz. The layer thickness of LaAlO$_3$ was *in situ* monitored by the RHEED (reflected high energy electron diffraction) technique. After deposition, the sample was annealed in 200 mbar of O$_2$ at 600 °C for one hour, and then cooled to room temperature in the same oxygen pressure.

Measurements. The structure of SrTiO$_3$ was measured in the presence of a gate voltage and light illuminating, by a Bruker diffractometer (D8 Discover, Cu K$_\alpha$ radiation) with the x-ray being sparallelized and monochromatized by an asymmetric Ge 2202-Bounce monochromator. A transverse electrical field was applied to the bottom electrode of SrTiO$_3$, while the top electrode was grounded. Lasers adopted in the present experiments have a wavelength between 532 nm and 980 nm. The spot size of the laser beam is 4 mm^2, focusing on the regions where the x-ray was reflected. Ultrasonic Al wire bonding (20 μm in diameter) was employed for electrode connection for the LaAlO$_3$/SrTiO$_3$ sample. The four welding spots were well aligned, and the separation between neighbouring spots was ~0.4 mm. Laser beam focused on the area between two inner leads. The applied current for conductance measurements was 1 μA. All data were acquired at ambient temperature.

References

1. Devonshire, A. F. Theory of ferroelectrics. *Phil. Mag. Suppl.* **3,** 85–130 (1954).
2. Haeni, J. H. *et al.* Room-temperature ferroelectricity in strained SrTiO$_3$. *Nature* **430,** 758–761 (2004).
3. Zubko, P., Catalan, G., Buckley, A., Welche, P.R. L. & Scott, J. F. Strain-gradient-induced polarization in SrTiO$_3$ single crystals. *Phys. Rev. Lett.* **99,** 167601 (2007).
4. Singh-Bhalla, G. *et al.* Built-in and induced polarization across LaAlO$_3$/SrTiO$_3$ heterojunctions. *Nat. Phys.* **7,** 80–86 (2011).
5. Rössle, M. *et al.* Electric-field-induced polar order and localization of the confined electrons in LaAlO$_3$/SrTiO$_3$ heterostructures, *Phys. Rev. Lett.* **110,** 136805 (2013).
6. Hanzig, J. *et al.* Migration-induced field-stabilized polar phase in strontium titanate single crystals at room temperature. *Phys. Rev. B* **88,** 024104 (2013).
7. P. Calvani *et al.* Observation of a midinfrared band in SrTiO$_{3-\delta}$. *Phys. Rev. B* **47,** 8917 (1993).
8. Schooley, J. F., Hosier, W. R. & Cohen, M. L. Superconductivity in semiconducting SrTiO$_3$. *Phys. Rev. Lett.* **12,** 474–475 (1964).
9. Hanzig, J. *et al.* Strontium titanate: An all-in-one rechargeable energy storage material. *Journal of Power Source* **267,** 700–705(2014).
10. Menesklou, W. *et al.* High temperature oxygen sensors based on doped SrTiO$_3$. *Sensors and Actuators B: Chemical* **59,** 184–189 (1999).
11. Walter, M. G. *et al.* Solar water splitting cells. *Chemical Reviews* **110,** 6446–6473 (2010).
12. Waser, R. & Aono, M. Nanoionics-based resistive switching memories. *Nat. Mater.* **6,** 833–840 (2007).

13. Stashans, A. & Vargas, F. Periodic LUC study of F centers in cubic and tetragonal SrTiO₃. *Mater. Lett.* **50,** 145–148 (2001).
14. Ricci, D., Bano, G., Pacchioni, G. & Illas, F. Electronic structure of a neutral oxygen vacancy in SrTiO₃. *Phys. Rev. B* **68,** 224105 (2003).
15. Cuong, D. D. *et al.* Oxygen vacancy clustering and electron localization in oxygen-deficient SrTiO₃: LDA + U study. *Phys. Rev. Lett.* **98,** 115503 (2007).
16. Lin, C. W. & Demkov, A. A. Electron correlation in oxygen vacancy in SrTiO₃. *Phys. Rev. Lett.* **111,** 217601 (2013).
17. Muller, D. A. *et al.* Atomic-scale imaging of nanoengineered oxygen vacancy profiles in SrTiO₃. *Nature* **430,** 657–661 (2004).
18. Wang, X. *et al.* Static and ultrafast dynamics of defects of SrTiO₃ in LaAlO₃/SrTiO₃ heterostructures. *Appl. Phys. Lett.* **98,** 081916 (2011).
19. Cordero, F. Hopping and clustering of oxygen vacancies in SrTiO₃ by anelastic relaxation. *Phys. Rev. B* **76,** 172106 (2007).
20. Souza, R. A. D., Metlenko, V., Park, D. & Weirich, T. E. Behavior of oxygen vacancies in single-crystal SrTiO₃: Equilibrium distribution and diffusion kinetics. *Phys. Rev. B* **85,** 174109 (2012).
21. Szot, K, Speier, W., Carius, R., Zastrow, U. & Beyer, W. Localized metallic conductivity and self-healing during thermal reduction of SrTiO₃. *Phys. Rev. Lett.* **88,** 075508 (2002).
22. Liu, Z. Q. *et al.* Metal-insulator transition in SrTiO₃₋ₓ thin films induced by frozen-out carriers, *Phys. Rev. Lett.* **107,** 146802 (2011).
23. Merkle, R., Souza, R. A. D. & Maier, J. Optically tuning the rate of stoichiometry changes: surface-controlled oxygen incorporation into oxides under UV irradiation. *Angew. Chem.* **113,** 2184–2187 (2001).
24. Mochizuki, S., Fujishiro, F. & Minami, S. Photoluminescence and reversible photo-induced spectral change of SrTiO₃. *J. Phys.: Condens. Mater* **17,** 923–948 (2005).
25. Thiel, S., Hammerl, G., Schmehl, A., Schneider, C. W. & Mannhart, J. Tunable quasi-two-dimensional electron gases in oxide heterostructures. *Science* **313,** 1942–1945 (2006).
26. Lu, H. L. *et al.* Photoelectrical properties of insulating LaAlO₃–SrTiO₃ interfaces, *Nanoscale* **6,** 736–740 (2014).
27. Lu, H. L. *et al.* Reversible insulator-metal transition of LaAlO₃/SrTiO₃ interface for nonvolatile memory, *Scientific Reports* **3,** 2870 (2013).
28. Zafar, S. *et al.* Oxygen vacancy mobility determined from current measurements in thin Ba₀.₅Sr₀.₅TiO₃ films. *Appl. Phys. Lett.* **73,** 175–177 (1998).
29. Many, A. & Rakavy, G. Theory of transient space-charge-limited currents in solids in presence of trapping. *Phys. Rev.* **26,** 1989 (1962).
30. Moos, R. & Härdtl, K. H. Defect chemistry of donor-doped and undoped strontium titanate ceramics between 1000°C and 1400°C. *J. Am Ceram. Soc.* **80,** 2549–2562 (1997).
31. Moos, R., Menesklou, W. & Hardtl, K. H. Hall mobility of undoped n-type conducting strontium titanate single crystals between 19 K and 1373 K. *Appl. Phys. A* **61,** 389–395 (1995).

Acknowledgements

Author Contributions

J.R.S. conceived and designed the experiments, and prepared the manuscript. Y.Li and Y.Lei conducted the experiments. B.G.S. oversaw the project. All authors commented on the manuscript.

Additional Information

Competing financial interests: The authors declare no competing financial interests.

How to cite this article: Li, Y. *et al.* Visible-light-accelerated oxygen vacancy migration in strontium titanate. *Sci. Rep.* **5**, 14576; doi: 10.1038/srep14576 (2015).